energies

MDPI

Article

Study of the NH_3-SCR Mechanism on $LaMnO_3$ Surfaces Based on the DFT Method

Dongdong Ren [1,*], Kai Wu [2], Siyi Luo [1,*], Yongjie Li [1], Keting Gui [3], Zongliang Zuo [1] and Xianjun Guo [4]

[1] School of Environmental and Municipal Engineering, Qingdao University of Technology, Qingdao 266520, China
[2] Technology Center, China Tobacco Jiangsu Industrial Co., Ltd., Nanjing 210019, China
[3] School of Energy and Environment, Southeast University, Nanjing 210096, China
[4] School of Environment and Material Engineering, Yantai University, Yantai 264005, China
* Correspondence: ren632477967@163.com (D.R.); luosiyi666@126.com (S.L.)

Abstract: $LaMnO_3$ with perovskite structure is a SCR de-NO_x catalyst with good performance at low temperatures. In this paper, the SCR reaction process on the 010 surface of $LaMnO_3$ catalyst was studied by DFT method, to guide the development of catalysts and their effective application. The results obtained through research indicate that both E-R and L-H mechanisms exist on the catalyst surface. The NH_3 molecule can be absorbed on L acid and then oxidized by lattice oxygen to form NH_2. Then, NH_2 can react with the NO molecule to form NH_2NO and decompose to N_2 and H_2O. The NH_3 can also be absorbed with hydroxyl to form NH_4^+, it can also react with NO to form NH_2NO and then decompose. The NH_4^+ also can react with NO_3^- which is formed by NO oxidized when O_2 is present, to participate in the rapid SCR process.

Keywords: $LaMnO_3$; NH_3-SCR; DFT; NO_x removal

Citation: Ren, D.; Wu, K.; Luo, S.; Li, Y.; Gui, K.; Zuo, Z.; Guo, X. Study of the NH_3-SCR Mechanism on $LaMnO_3$ Surfaces Based on the DFT Method. *Energies* **2022**, *15*, 9099. https://doi.org/10.3390/en15239099

Academic Editor: Jacek Grams

Received: 18 October 2022
Accepted: 27 November 2022
Published: 30 November 2022

1. Introduction

NO_x (Nitrogen oxide) is a common air pollutant widely present in nature and human industrial activity [1]. It not only does harm to people health, but also causes great damage to the ecological environment [2]. Due to the extensive combustion of fossil energy such as coal, a large amount of NO_x is discharged into the atmosphere every year [3]. According to statistics, more than 75% of NOx in the atmosphere is produced by human activities, and this value is increasing year by year [4]. To meet the challenge of NO_x emissions, many countries and international regions have limited NO_x emissions and proposed various de-NO_x technologies [5]. SCR (selective catalytic reduction) is one of the most widely used de-NO_x technologies. It is mature, stable, and efficient with activity reaching 80–95%, and can meet de-NO_x requirements under different conditions in various production contexts [6].

SCR refers to the process of reducing NO to N_2 with reducing gases such as NH_3 and CO under the action of a catalyst; the reaction equation is known to be $4NO + 4NH_3 + O_2 \rightarrow 4N_2 + 6H_2O$ [7]. The catalyst is the core component, and the quality of catalyst directly determines the de-NO_x performance. At present, V_2O_5-WO_3/TiO_2 catalysts are widely used in commercial activities. The active temperature window of this kind of catalyst is 300–400 °C, which provides high de-NO_x efficiency and stability [8]. However, the high active temperature is not suitable for de-NO_x in the flue-gas tail, and the crystal form of anatase TiO_2 is unstable, which hinders its regeneration application. Furthermore, V_2O_5 has biological toxicity [9]. Therefore, it is imperative to actively develop environmentally friendly de-NO_x catalysts with high efficiency at low temperatures.

Perovskite materials have the advantages of good structural stability, high-temperature sintering resistance, strong chemical adsorption capacity, rich acid–base sites, easy regulation of redox properties, rich reserves, and low price [10]. To date, many researchers

have studied the structure–activity relationship of perovskite catalysts and their SCR properties [11]. Perovskite is the general name given to oxides with stable cubic ABO_3 structure, the A-site ion is a rare earth metal or alkaline earth metal cation with large radius and the B-site ion is a transition metal cation [12].

$LaMnO_3$ perovskite oxides, in which La as the A site plays a supporting role while Mn as the B site is the main active site, have strong stability and good SCR activity. They have great potential as low-temperature catalysts, which has attracted the attention of many scholars [13]. Zhang tested the de-NO_x performance of $LaMnO_3$ catalysts, and the results showed that $LaMnO_3$ perovskite exhibited excellent catalytic activity in the SCR of NO using NH_3, and the NO conversion could reach 78% at 250 °C, increasing along with the temperature in the range of 100–300 °C [14]. Guo et al. prepared $LaMnO_3$ catalysts and carried out modification and activity testing. The results showed that the modified catalyst demonstrated excellent activity with 90% NO_x conversion at 135 °C and more than 90% NOx conversion in the temperature window of 135–260 °C [15]. Wang et al. prepared $LaMnO_3$ supported iron ore catalysts by citric acid complex impregnation and tested SCR activity, and the results showed that the NO_x conversion efficiency was up to 98% at 180 °C [16]. These results fully demonstrate the good catalytic performance of SCR. However, the mechanism of the NO_x conversion reaction with the $LaMnO_3$ catalyst is still not clear yet.

Understanding the reaction mechanism on the catalyst surface is of great significance to the development of the SCR catalyst. In general, there are two kinds of NH_3-SCR reaction mechanisms. One is the L-H (Langmuir–Hinshelwood) mechanism, in which NH_3 and NO are adsorbed on the catalyst surface, and react to form products, and the other is E-R (Eley–Rideal) mechanism in which NH_3 is mainly adsorbed on the catalyst surface and then reacts with gaseous or weakly adsorbed NO [17,18]. Yang et al. studied the mechanism of a Fe-Mn mixed oxide catalyst with a spinel structure by in situ drift experiment, and reported that both the L-H mechanism and the E-R mechanism were active on the catalyst surface, the E-R mechanism dominant at high temperature and the L-H mechanism at low temperature [19]. Zhang et al. studied Mn based perovskite catalysts with Bi and La at position A, and found that the perovskite catalyst had strong Lewis acid (L-acid) and rich concentration of surface oxygen, which may have been the reason for the strong catalytic activity [20]. Further study by Zhang et al. on the mechanism of the $LaMnO_3$ catalyst showed that the excellent de-NO_x performance of $LaMnO_3$ lies in the large NH_3 adsorption capacity and rich nitrate or nitrite species. They proposed an L-H mechanism in which gaseous NH_3 and NO are adsorbed in the form of NH_4^+ ions and nitrosyl species, respectively, and then oxidized to nitrite and nitrate. Then, NH_4^+ reacts with active nitrite to produce unstable ammonium nitrite, and finally N_2 [14]. However, some researchers believe that the two mechanisms exist at the same time [21]. The study of $LaBO_3$ perovskite material (B = Mn, Ni, Fe, CO) by Shi et al. showed that its catalytic activity has no significant relationship with its reduction ability, but follows the same law as the adsorption capacity of NH_3 [22]. It can be considered that the adsorption capacity of NH_3 plays an important role in NH_3-SCR. However, it should be noted that in the field of perovskite NH_3-SCR de-NO_x, the mechanism research is still relatively simple, the catalytic processes of perovskite materials in different systems are different, and no consensus has been reached so far [23].

With the development of theoretical chemistry and computer technology, first principles and density function theory (DFT) have been introduced in the field of catalyst mechanism research by various researchers. Soyer et al. [24] used a quantum chemical method to study the mechanism on the V_2O_5 catalyst surface. Their results showed that the B acid site on the catalyst surface is the main reaction center, NH_3 combines to form NH_4^+, and reacts with NO to finally produce N_2 and H_2O. Yang et al. [25] studied the reaction pathway on the CeO_2/TiO_2 catalyst surface by applying DFT, and their results showed that NH_3 is first coordinated and adsorbed on the surface L acid site in molecular form, then activated by dehydrogenation to generate NH_2, and then reacts with NO to

generate N_2 and H_2O, following the E-R mechanism. Li et al. [26] studied the reaction on the Mn/γ-Al_2O_3 surface, the results showing that there were L acid and B acid sites on the catalyst surface at the same time, and that NH_3 can be adsorbed on the L acid site, and then dehydrogenated to NH_2. The NH_2 fragment reacts with NO to produce NH_2NO which is then decomposed to produce N_2 and H_2O. At the same time, NH_3 is also adsorbed on the B acid site to form an NH_4^+ cation, then it can react with NO_2 to form NH_4NO_2, and finally decompose to form N_2 and H_2O, which shows that there are both E-R and L-H mechanisms on the Mn/γ-Al_2O_3 surface. Anstrom et al. [27] also studied the mechanism on the surface of vanadium oxide catalyst and reported that NH_2NO is the main intermediate product. These experiments fully prove the correctness of the first principle and the DFT calculation. At present, there is no definite conclusion on which mechanism is dominant on different catalyst surfaces, but the results obtained through DFT can help to a certain extent reveal it and make up for the deficiency of calculations.

Scholars are also conducting research on the first principle and DFT of perovskite catalyst. Zhang et al. calculated the atomic charges of $BiMnO_3$ and $LaMnO_3$ through DFT and found that the smaller O charge and higher electronegativity brought stronger acidity, promoted the adsorption and activation of NH_3 on the surface, and increased low-temperature NH_3-SCR activity [20]. Yan et al. studied the CO-SCR reaction process on the surface of $LaMnO_3$ catalyst, obtained the basic steps, activation energy barrier, and other parameters, and determined the surface reaction path [28]. Meanwhile, DFT-based study on NH_3-SCR surface reaction on $LaMnO_3$ catalyst has not been reported.

In conclusion, $LaMnO_3$ catalyst with perovskite structure is a good low-temperature SCR de-NO_x catalyst, but the research on its mechanism is relatively shallow. Using a mature and reliable DFT method to study the reaction process is helpful to reveal its surface reaction mechanism and guide the development and application of low-temperature de-NO_x catalysts. Therefore, in this study, the DFT method was applied to study the surface reaction mechanism, and parameters including the molecular adsorption process, elementary reaction steps, and activation energy were measured. The adsorption behavior and reaction process were studied, and the most probable reaction path on the catalyst surface was identified.

2. Computational Methods and Models

In this paper, the $LaMnO_3$ catalyst as research object is established; its structure is shown in Figure 1. Figure 1a shows the supercell of the $LaMnO_3$ catalyst, and Figure 1b shows its 010 surface. The $LaMnO_3$ catalyst is an orthorhombic structure with a Pnma space group [28], shown in Figure 1a, where the pale blue spheres represent La elements, occupying the A position and playing the role of the supporting structure, and the purple indicates that the Mn ion is the main reactive site. The (010) surface of $LaMnO_3$ is particularly thermodynamically stable [29]. Therefore, the 010 surface of $LaMnO_3$ catalyst was selected as the active surface to establish the model and calculations. Experiments have shown that the 010 surface with Mn as the terminal has better stability than the La-terminated surface [30]. Moreover, Mn as the active site can play a better catalytic role when exposed to the surface. A surface with Mn is generally used as the terminal in practical applications [31]. Therefore, the Mn-terminated 010 surface of $LaMnO_3$ catalyst was established in this research model, as shown in Figure 1b. Figure 1b shows a p(2×2) supercell, Mn cations are exposed to the surface as the main active site. The established model was a periodic plate structure. To simplify the calculation, we chose a 2×1 model for calculation [32]. Due to the number of layers of the grid having little effect on the results, a three-layered structural grid was established, the bottom atoms fixed and the two surface layers relaxed and optimized [33]. A vacuum layer with 30 Å was added to the lattice to eliminate the interaction between adjacent layers.

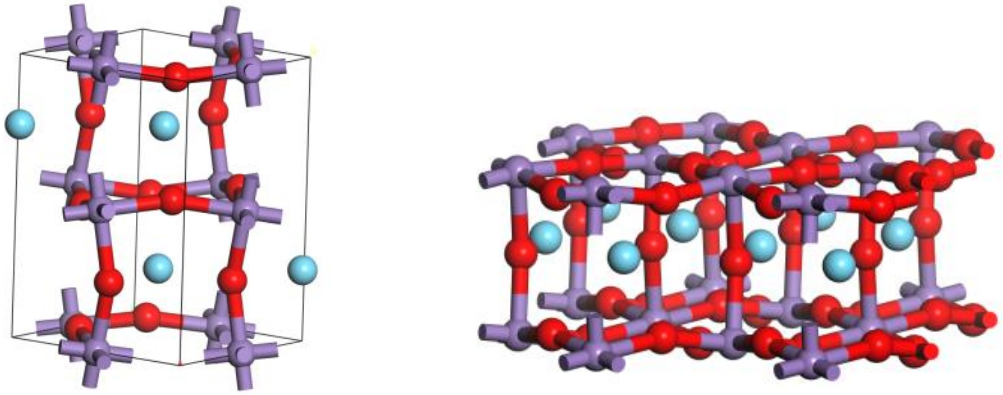

Figure 1. The conventional cell and (0 0 1) surface of $LaMnO_3$. (**a**) the conventional cell of $LaMnO_3$, (**b**) the (0 0 1) surfac of $LaMnO_3$ (red spheres, purple spheres, and pale blue spheres represent the O anions, Mn cations, and La cations, respectively).

The Dmol3 program package was employed in the calculation process. In order to describe the electron exchange potential energy, the GGA (generalized gradient approximation) function was selected [34]. The internal electrons of Mn and La atoms were processed using the effective nuclear potential (ECP) method to facilitate the calculation [35]. The numerical orbit basis was selected as the basic function to solve the DFT equation. The number of atomic orbitals is controlled by the double numerical basis set of polarization function (DNP) [36]. The cut-off numerical basis set value was 4.4 Å.

In the SCR process, small molecules such as NH_3 can be absorbed on the surface, and the absorption strength is evaluated by the adsorption energy, which is defined in the equation [37]:

$$E_{ads} = E_{slab+molecule} - E_{slab} - E_{molecule} \quad (1)$$

where E_{ads}, $E_{slab+molecule}$, E_{slab}, and $E_{molecule}$ represent the adsorption energy, total energies of the substrate plus small molecules, the energy of substrate surface, and the energy of small molecules, respectively.

In the reaction process, there are intermediate, final, and transition states in each elementary reaction. The transition state of each reaction step was obtained by the linear synchronous transition quadratic synchronous transition (LST-QST) method, and only one virtual frequency was ensured [38]. The Brillouin zone sampling was set to ($3 \times 3 \times 1$) on a Monkhorst–Pack k-point grid. The convergence criteria were defined as atomic force 4.0×10^{-3} Hartree/Å, maximum displacement 5.0×10^{-3}Å, total energy variation 2.0×10^{-5} Hartree, and the self-consistent field (SCF) tolerance was 1.0×10^{-5} Hartree [37].

The activation energy barrier (Ea) is defined by the following equation [39]:

$$\mathrm{Ea} = \mathrm{E_{TS}} - \mathrm{E_{IM}} \quad (2)$$

where E_{TS} and E_{IM} represent the total energy of transition state and intermediate state, respectively.

3. Results and Discussion

3.1. Reaction of L Acid

On the surface of $LaMnO_3$, there are Mn cations which are active sites that distribute L acids, and these sites can accept lone pair electrons provided by MH_3. Zhang's experiment fully proved this [14]. Figure 2 shows the adsorption configuration of NH_3, and the corresponding parameters are listed in Table 1.

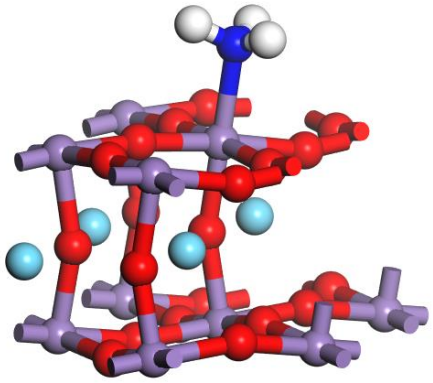

Figure 2. The adsorption configuration of NH_3.

Table 1. The parameters of optimized NH_3 adsorption configuration.

Mn–N Bond Length (Å)	Angle of N–H (°)	Mulliken Charge of NH_3 (a.u)	Adsorption Energy (kJ/mol)
2.107	109.782	0.327	−97.9

In this situation, the N atom of NH_3 bonds to the Mn site and conforms to a stable configuration with a bond length of 2.107 Å. The average angle of N-H is 109.782°, compared with 107° when not adsorbed. The angle increases due to the electron transfer from NH_3 to the $LaMnO_3$ surface, as the Mulliken charge of NH_3 is 0.327, meaning there are electrons transferred from NH_3 to the surface. It can be inferred that the lone pair electrons of NH_3 could be contained by the empty orbits of $LaMnO_3$, and this property leads to electron migration. The same activity has also been observed on the surfaces of other Mn based catalysts [32].

In order to explore the adsorption mechanism, the partial density of state (PDOS) was assessed and the results are shown in Figure 3. In the figure, various orbitals of the NH_3 molecule and Mn ion are shown. A strong formant peak is visible at about −4 eV between the p orbit of NH_3 and the p and d orbits of the Mn cation, which means that there a strong bond has been formed. Furthermore, there is also a relatively weak peak at −5.5 eV between the p orbit of NH_3 and the s orbit of the Mn cation, indicating the formation of a bond between the two. These results show that the NH_3 molecule could absorbed on the Mn cation as the main active site in the SCR process, fully demonstrating that the $LaMnO_3$ catalyst is sufficient active. The adsorption behavior has an important influence on the subsequent reactions.

There are full experimental results that show that NH_3 undergoes dehydrogenation after adsorption on different catalyst surfaces, whether with the L-H mechanism or E-R mechanism [40]. By comparing and analyzing the various possibilities after adsorption of NH_3, it can be concluded that the dehydrogenation reaction can also still happen. Figure 4 shows the diagram of potential energy and the optimized structures of the NH_3 dehydrogenation reaction. It can be seen that the dehydrogenation process is divided into two stages. In the first step, one of the H atoms is attracted by lattice oxygen on the surface and NH_2 is formed. The active energy barrier is 22.5 kcal/mol, this value is close to the surface of γFe_2O_3 which is 22.010 kcal/mol [37], but lower than those of CeO_2/TiO_2 and V-based catalysts, 37.77 kcal/mol and 63.6 kcal/mol, respectively [41,42]. This may be due to the similar chemical properties of the Fe cation and Mn cation. The reaction heat of the step is 12.4 kJ/mol, which means that it is an endothermic reaction. This is because the breaking of the NH bond absorbs energy, and the energy released by the combination of lattice oxygen and H is not enough to compensate for it. It is the same case on the surface of Fe_2O_3, but the reaction heat is lower [37] and that means the process is easier to carry out. The next step is that the NH_2 continues to lose one H atom to the lattice oxygen and

forms an NH segment. The active energy barrier is 31.8 kcal/mol and the reaction heat is 19.6 kcal/mol. The barrier is higher than in the previous step, which means the process is more difficult to carry out, so NH is less likely to occur. This may be because there are three stable chemical bonds around the N, making NH_2 on the Mn site a relatively stable configuration so that the H is difficult to remove, which is the case for other catalyst surfaces [32,37]. The reaction heat has a positive value which means the reaction is also an endothermic reaction. Therefore, NH_2 is the main product after the adsorption of NH_3, with a small amount of NH.

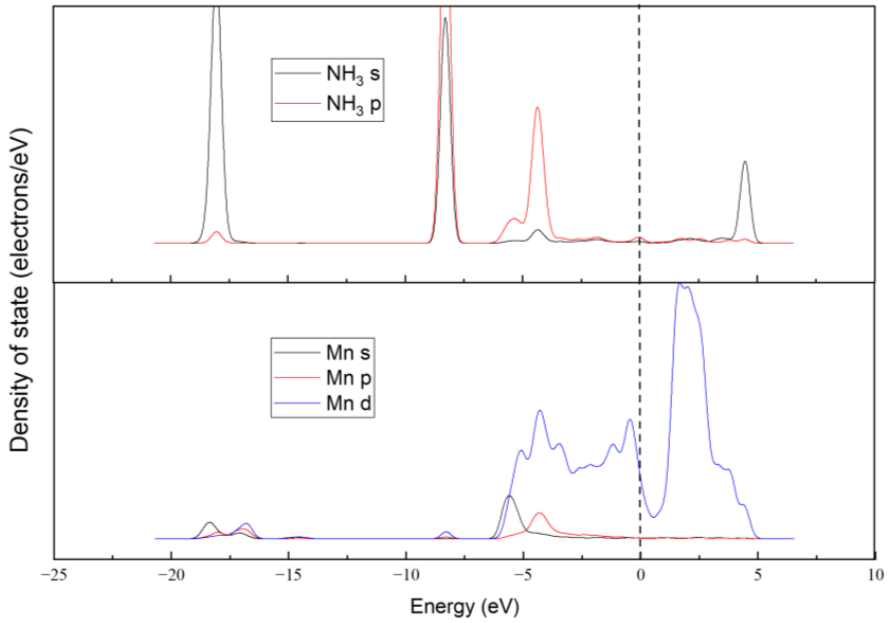

Figure 3. The partial density of state for NH_3 adsorption configuration.

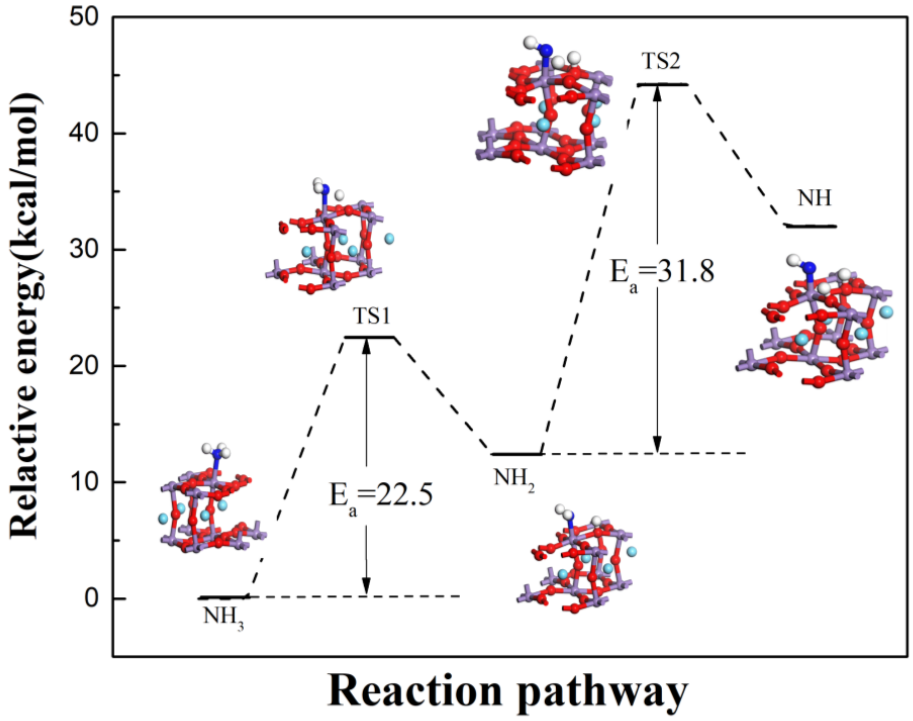

Figure 4. Process of the NH_3 dehydrogenation reaction.

According to the E-R mechanism, NH_2 is the main intermediate product in the SCR process, which can form NH_2NO and then decompose [38]. By analyzing the reaction pathway on the $LaMnO_3$ catalyst surface, it has been observed that such a reaction path exists, as shown in Figure 5. The reaction pathway in the figure is divided into the formation and decomposition of NH_2NO. The active energy barrier and reaction heat in the first step are 0.1 kcal/mol and −2.7 kcal/mol. The reaction is an exothermic reaction due to the reaction heat being a negative value because energy is released during the N-N bonding process. The energy barrier is so small as to be negligible, which means the NH_2NO forms very easily because the movement of NO to the surface encounters only minimal resistance.

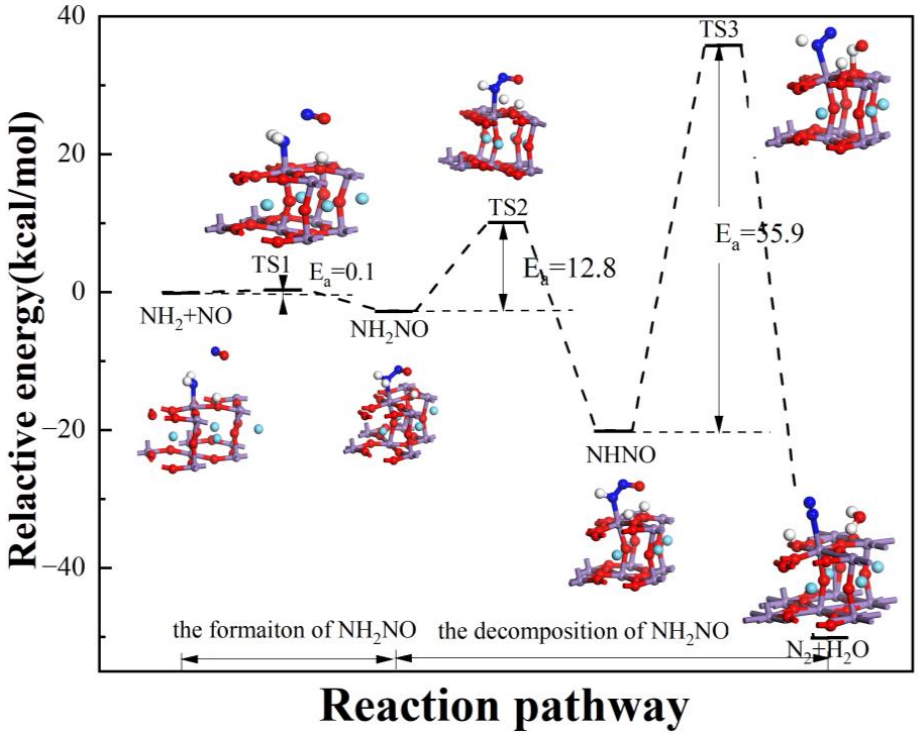

Figure 5. The reaction process of NH_2NO formation and decomposition reaction over catalyst.

The next step reaction is the composition of NH_2NO, and is also divided into two steps. The first is removal of one H atom from NH_2NO under the action of lattice oxygen, where the active energy barrier is 12.8 kcal/mol. The barrier is much lower compared with previous dehydrogenation processes, because the formation of the N-N bond means N has a high coordination number so the H atom link is not very tight, making it easy to remove. The reaction heat was reported as −17.4 kcal/mol, which means it is also an exothermic reaction. This is because H needs less energy in the process of removal and releases energy in the process of combining with lattice oxygen. The second step is the NHNO decomposition to N_2 and H_2O. The active energy barrier is 55.9 kcal/mol and the reaction heat is −29.9 kcal/mol. In the process, the N-O breaks and the O atom is combined with two H atoms which had been removed in previous steps, forming a H_2O molecule. In addition, the last H atom separates from the N atom and bonds to lattice oxygen and is left on the surface at the end. At the same time, a triple bond is formed between two N atoms to form N_2 as a stable gas as the final product. Compared with previous steps, the energy barrier is higher because the breaking of N-O bond requires considerable energy, and the phenomenon is the same as on the surface of Mn-based catalyst [43,44]. The reaction is also an exothermic reaction, because of the amount of energy released in the N_2 formation process.

Briefly, the SCR process includes the dehydrogenation process, the formation of NH_2NO, and the decomposition of NH_2NO. The whole process is similar those on the

Fe-based, V-based, and Mn-based catalyst surfaces [37,42,43]. In the reaction process shown in Figures 4 and 5, the determining step is the decomposition of NHNO because of it has the highest energy barrier. There is no O_2 involved in this reaction process, which means that the SCR process could be carried out in an anaerobic environment and that the lattice oxygen plays an important role. One H atom remains left at the end and needs to be oxidized, so O_2 is necessary in the SCR process.

When O_2 exists in the atmosphere, it can be absorbed on the surface. The absorption configuration is shown in Figure 6, and the corresponding parameters are listed in Table 2. The data show that the O_2 can be absorbed on the Mn site, and one O atom combines with the Mn cation to form a stable chemical bond with a bond length of 2.015 Å. In the process, the adsorption energy is −47.9 kJ/mol, referring to the amount of energy released because of the Mn-O bond formed. There are many electrons transferred from base to O_2 molecule, indicated by the Mulliken charge of −0.129 a.u. reflecting the strong oxidation of O_2. The O-O bond length after adsorption was shown to be 1.268 Å, compared with 1.208 Å before adsorption. This may be caused by the increase of charge density around the O_2, caused by electron immigration.

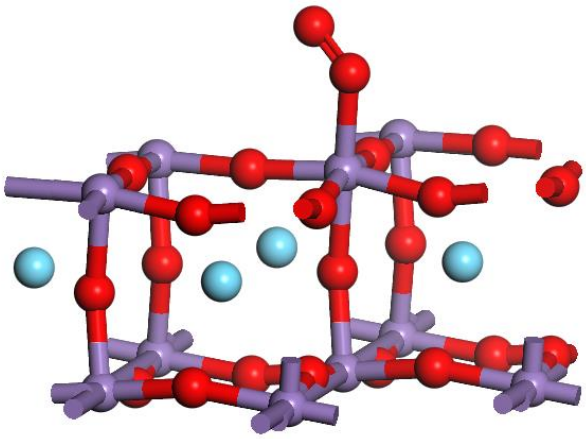

Figure 6. The absorption configuration of O_2 on $LaMnO_3$ catalyst surface.

Table 2. The parameters of O_2 adsorption configuration.

Mn–O Bond Length (Å)	O–O Bond Length (Å)	Mulliken Charge of O_2 (a.u)	Adsorption Energy (kJ/mol)
2.015	1.268	-0.129	−47.9

The partial state density is analyzed in Figure 7. An obvious peak in Fermi energy level can be seen that at 0 eV between the p orbit of the O atom and d orbit of the Mn cation. This demonstrates that the two formed a strong resonance and formed a chemical bond. Furthermore, there are also two peaks at about −6 eV and −7 eV between O and Mn, corresponding mainly with the p orbital of O and the d orbital of Mn. Therefore, a stable resonance hybrid peak was formed between O and Mn, which should belong to a stable chemical adsorption process.

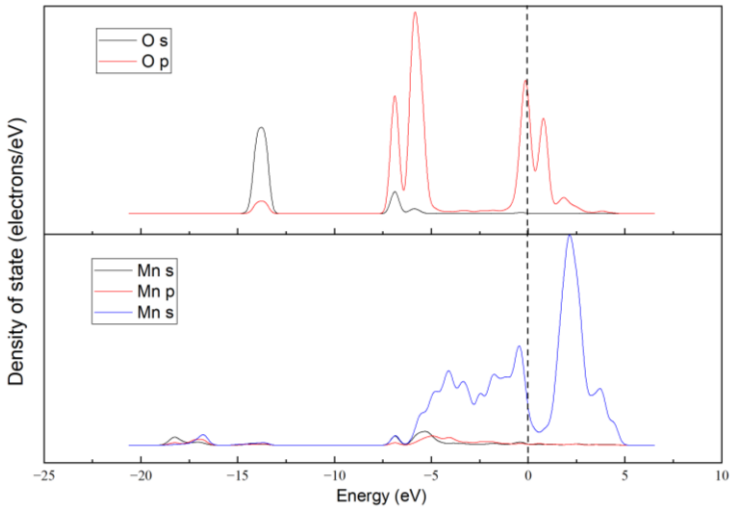

Figure 7. The partial density of state of O_2 adsorption configuration.

After the adsorption, the O_2 can decompose into two active O atoms on the surface which is shown in Figure 8. In the process, the chemical bond of the O_2 molecule is broken and divided. The originally free O atom is attracted by another Mn active site. Thus, two active O atoms are on the Mn site. The active O can oxidize the H atom left previously and form H_2O so as to leave the surface activity of the catalyst unaffected. Furthermore, the active O can also participate in the dehydrogenation of NH_3. The reaction heat was −3.9 kcal/mol, which means it is an exothermic reaction, because the Mn-O formation can release energy to compensate for the break of O_2 bond.

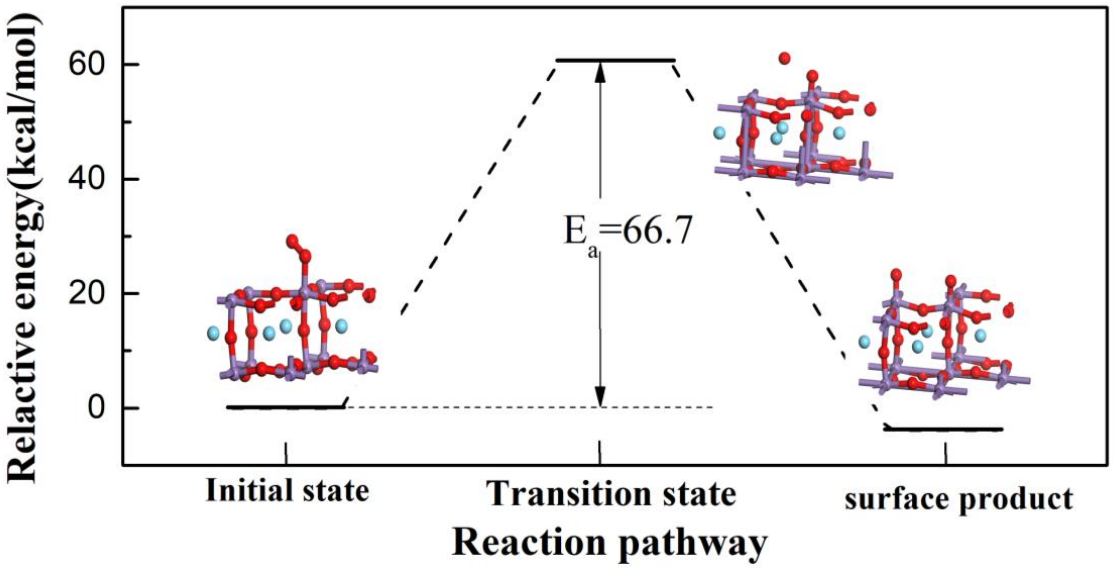

Figure 8. The decomposition process of O_2 on the $LaMnO_3$ surface.

The dehydrogenation of NH_3 under active oxygen is shown in Figure 9. The active energy barrier is 77.3 kcal/mol and the reaction heat is 10.1 kcal/mol. The energy barrier is much greater than 22.5 kcal/mol because of the effect of lattice oxygen. This maybe because the lattice oxygen is closer to the H atom than the active O. Thus, it can be inferred that the dehydrogenation of NH_3 mainly occurs under the action of lattice oxygen. This is very different from on the Fe_2O_3 catalyst surface. As previously, the reaction is again an endothermic reaction.

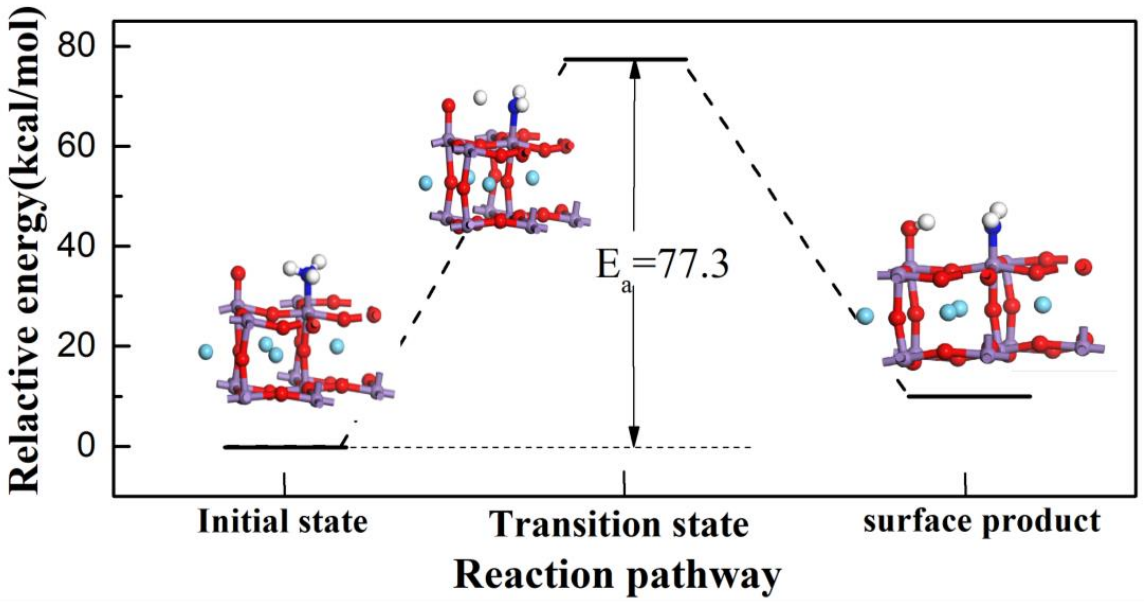

Figure 9. The dehydrogenation process of NH_3 under the action of active O oxygen.

Whether NH_2 can continue to be oxidized and dehydrogenated under the action of active O was also addressed, and the process is indicated in Figure 10. The active energy barrier was found to be 100.5 kcal/mol and the reaction heat was 10.4 kcal/mol. It can be seen that the active energy was much higher than in the previous example of dehydrogenation, which means that NH is not easy to generate in this state.

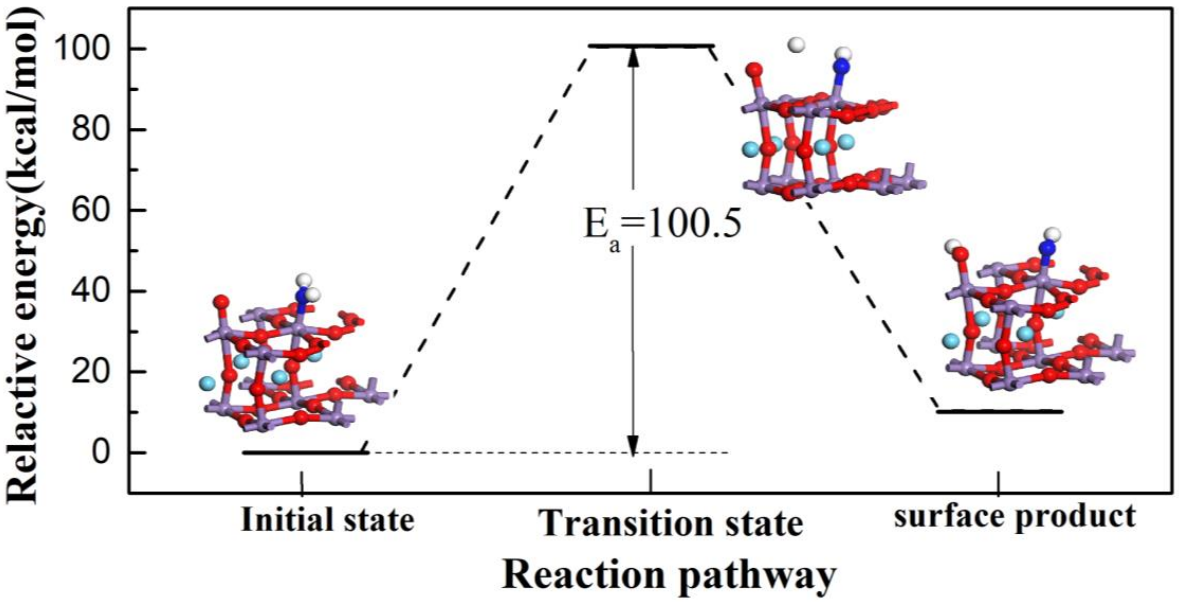

Figure 10. The dehydrogenation process of NH_2 under the action of active O oxygen.

Under aerobic conditions, there are NO_2 mechanisms that speed up the SCR process. The formation of NO_2 is shown in Figure 11. In this step, the active energy barrier is 0.1 kcal/mol which is as low as negligible. The reaction heat is −14.9 kcal/mol, meaning it is an exothermic reaction. The NO molecule in the atmosphere is located near active O on the catalyst surface, and N atoms are linked with O to form NO_2 and release energy.

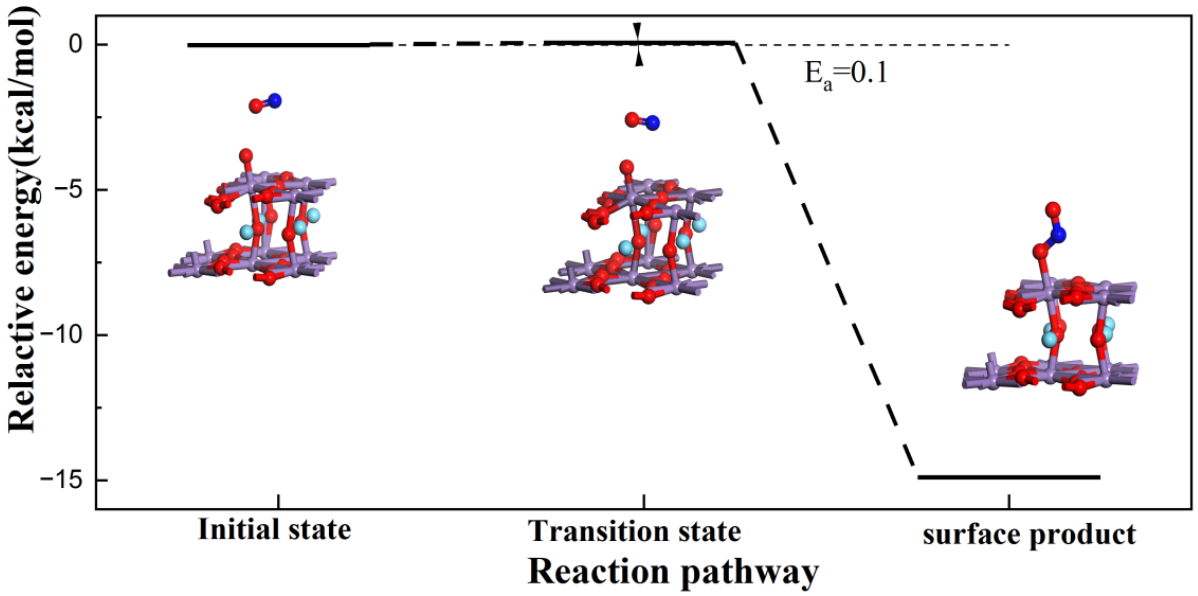

Figure 11. The formation process of NO_2.

The NO_3^- is the main product of the fast SCR mechanism, and the formation of NO_3^- is illustrated in Figure 12. The formed NO_2 overcomes a small potential barrier and approaches another O, so that N atoms combine with it to form NO_3^-. The active energy barrier is 0.6 kcal/mol and the reaction heat is −18.9 kcal/mol, which means it is also an exothermic reaction because the formation of the N-O bond releases energy.

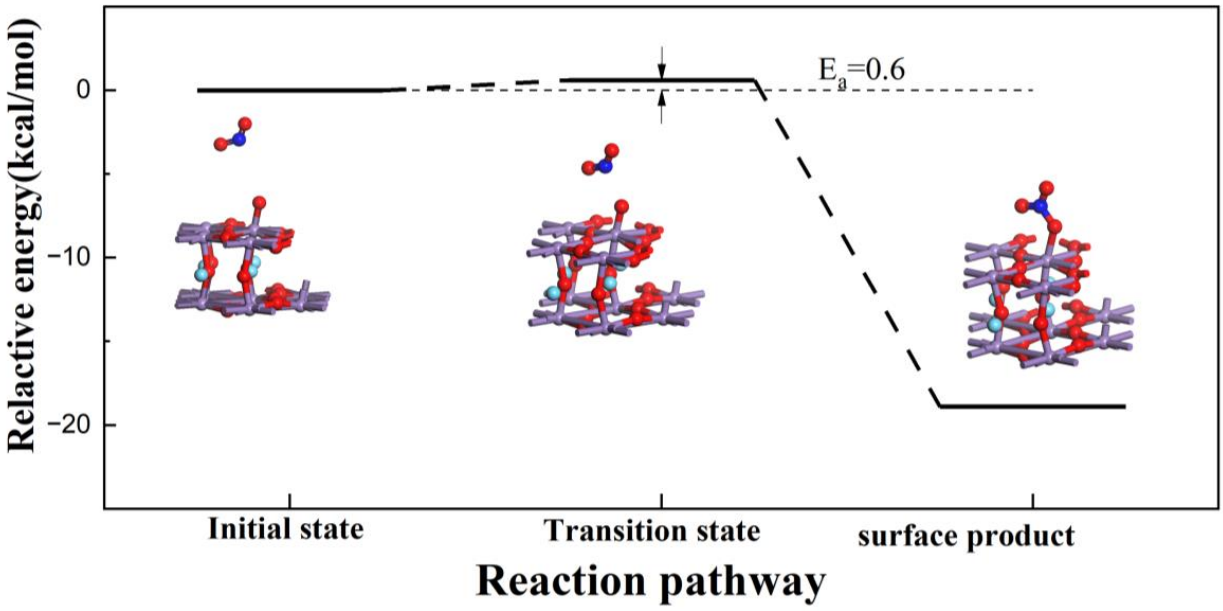

Figure 12. The formation process of NO_3^-.

It can be seen that the energy barriers formed by NO_2 and NO_3^- are sufficiently low so NO_3^- is easily formed. When there are NH_4^+ ions on the surface, they easily combine to form NH_4NO_3, and can then participate in the rapid SCR process as previously described [45,46]:

$$NH_4NO_3 + NO \leftrightarrow NH_4NO_2 + NO_2$$

$$NH_4NO_2 \rightarrow N_2 + 2H_2O$$

The NH_4NO_3 can react with NO and be reduced to NH_4NO_2 at 170 °C, and NH_4NO_2 can decompose to N_2 and H_2O at 100 °C. This reaction is easy to carry out, so it is known as a rapid reaction process and referred to as the L-H mechanism. On the $LaMnO_3$ surface, the easy formation of NO_3^- means that it is easy to achieve a rapid SCR reaction process, demonstrating that the $LaMnO_3$ catalyst has excellent low-temperature catalytic activity.

In summary, the O_2 can be absorbed and decomposed on the $LaMnO_3$ catalyst surface, and active O oxidation to NH_3 is not obvious. The main influence of oxygen is to oxidize NO to form NO_2 and NO_3^-, thus participating in the rapid SCR reaction process.

3.2. Reaction Process on B Acid

Following the previous steps, it can be seen there are H ions remaining on the surface that form a B acid. The NH_3 molecule can be absorbed on the B acid to form NH_4^+. Due to different forms of O on the catalyst surface, different hydroxyl forms may be present, and ammonium NH_4^+ ions exist in different forms, as shown in Figure 13.

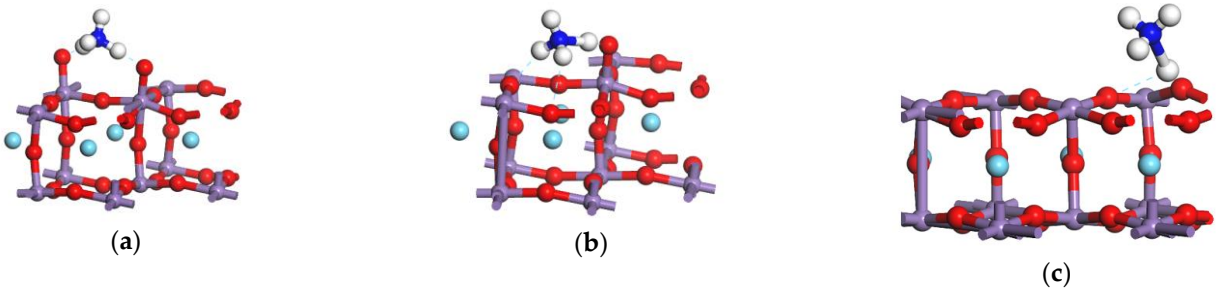

(**a**) (**b**) (**c**)

Figure 13. The configuration of NH_4^+ on the $LaMnO_3$ surface. (**a**) on two active O (**b**) on one active O (**c**) on lattice O.

In Figure 13a, there are two active O atoms on the surface, and two H ions bond to the two ions, while there is only one active O on the (b) configuration and none on the (c). The NH_4^+ ion connect with the active O in (b) and meanwhile act with the lattice oxygen, while NH_4^+ ions act only with surface lattice oxygen in (c). In addition to participating in the rapid SCR reaction with NO_3^-, surface NH_4^+ ions also react with NO to generate NH_2NO and decompose. The reaction process is shown in Figures 14–16.

Figure 14 shows the reaction process of the NH_4^+ ion in the Figure 13a configuration over the catalyst. The first step is that the NO moves to the surface and reacts with NH_4^+ to form NH_2NO. In this step, two H atoms that were connected to active O in the form of hydrogen bonds break off. The active energy barrier is 25.7 kcal/mol and the reaction heat is −13.1 kcal/mol. Compared with the L acid site, the energy barrier is a little higher and the reaction is an exothermic reaction. After the formation of NH_2NO, the surface ON fragment twists under the action of the surface, and the O atom is inclined to the side near the surface hydroxyl group. The NH_2NO species move slightly towards the surface, one H atom close to the lattice oxygen and another H atom close to the hydroxyl. The energy barrier is 9.4 kcal/mol, which means the reaction is easy to carry out, and the reaction heat is 0.1 kcal/mol. In this step, one H atom moves close to the hydroxyl and can react in the next step to form H_2O which is absorbed by the Fe cation. This represents the next process of NHNO formation, where the energy barrier is 3.4 kcal/mol and the reaction heat is −6.3 kcal/mol, indicating that the step is easy to achieve. On the NHNO configuration, the left H atom is close to the O atom so it easily reacts with it, and after the formation of NHNO, it can easily decompose. It can be seen that the H and O atoms can break away and bond, the H atom belonging to the hydroxyl also bonding to the O and forming a H_2O atom and also a N_2 molecule as the final product. The energy barrier is 8.1 kcal/mol and the reaction heat is −42.5 kcal/mol. The energy barrier is low and considerable energy is released during the process of N_2 and H_2O formation. The highest energy barrier in the whole process is the formation of NH_2NO which is as high as 25.7 kcal/mol, the others being sufficiently low, so the first step is the rate-determining step.

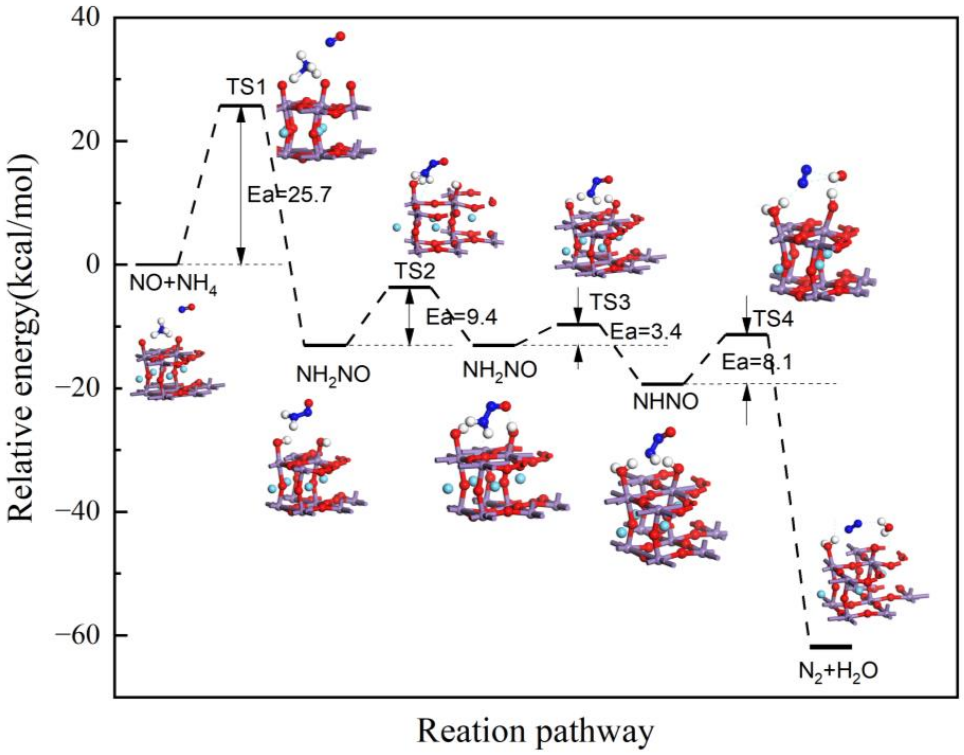

Figure 14. The NH_4^+ reaction process in the Figure 13a configuration over the catalyst.

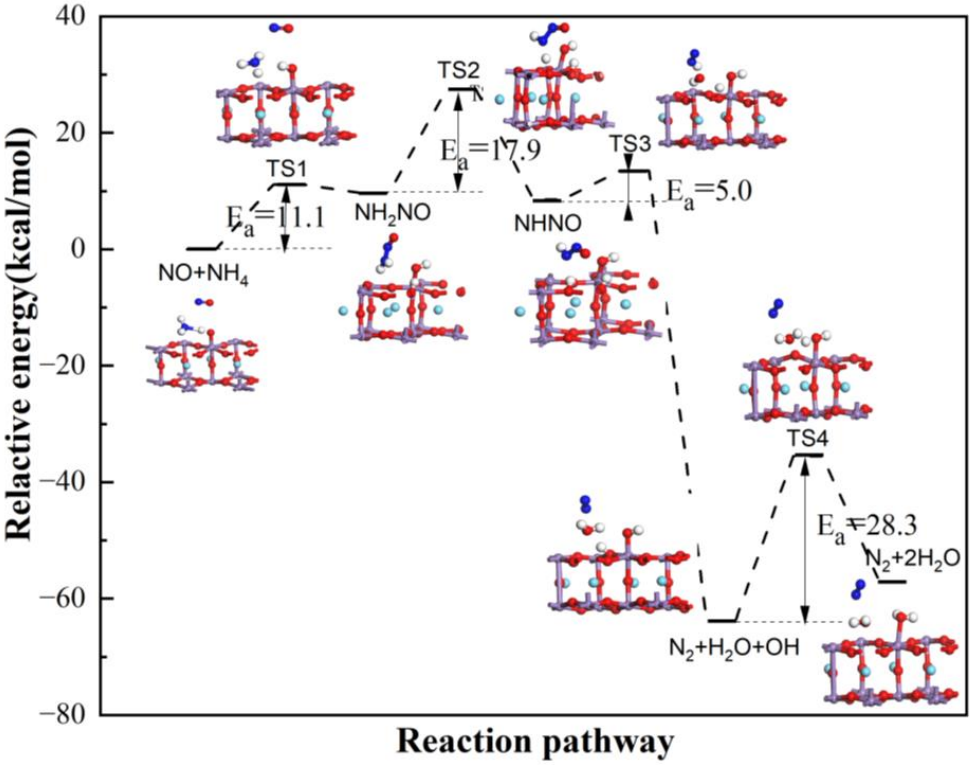

Figure 15. The NH_4^+ reaction process in the Figure 13b configuration over the catalyst.

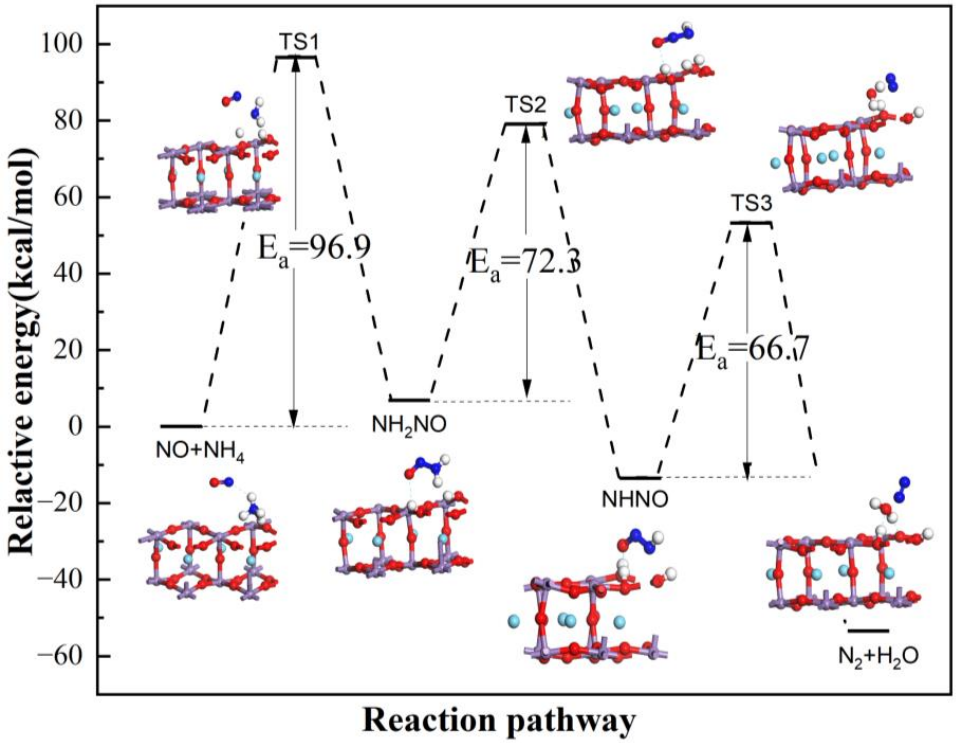

Figure 16. The NH_4^+ reaction process in the Figure 13c configuration over the catalyst.

Figure 15 shows the reaction process of the NH_4^+ ion in the Figure 13b configuration over the catalyst. There are four steps in the process. The first step is again the formation of NH_2NO. The active energy barrier was 11.1 kcal/mol and the reaction heat was 9.7 kcal/mol. Unlike in the previous pathway, this step was an endothermic reaction, which may be because of the breaking of two N-H bonds that need to absorb energy. After the formation of NH_2NO, one H atom was lost to produce NHNO, the energy barrier was 17.9 kcal/mol and the reaction heat −1.2 kcal/mol. This reaction is also easy to produce. Next, the O atom on NHNO can twist and bond to two H atoms on the NHNO and lattice oxygen to produce H_2O. Thus, the N_2 atom and one H_2O atom are formed in this step. The energy barrier is 5.0 kcal/mol and the reaction heat −72.3 kcal/mol. Significant energy is released because of the formation of N_2 and H_2O. There are also a hydroxyl and a H atom remaining, which could react to form H_2O. The energy barrier and reaction heat were respectively 28.3 kcal/mol and 6.7 kcal/mol. This represents another exothermic reaction. The highest energy barrier in the whole process is 28.3 kcal/mol and the reaction is a rate-determining step. For all that, relative values were not very high, so the pathway is easy to produce.

Figure 16 shows the reaction process of NH_4^+ ion in the Figure 13c configuration over the catalyst. There are three steps in the process, respectively the formation of NH_2NO, the formation of NHNO, and the decomposition of NHNO. The active energy barriers were 96.9 kcal/mol, 72.3 kcal/mol, and 66.7 kcal/mol. Compared with the highest barriers of 25.7 kcal/mol on Figure 14 and 28.3 kcal/mol on Figure 15, every step barrier was much higher, especially the first step which reached 96.9 kcal/mol. This was caused by the fact that active O on the surface has stronger activity than lattice oxygen. This also shows the role of O2 in promoting the SCR reaction. Due to the existence of active O, the activation energy of each step of the subsequent NH_4^+ reaction is greatly reduced. The respective reaction heats of each step are 6.8 kcal/mol, −20.1 kcal/mol, and −40.0 kcal/mol. The first step is an endothermic reaction and the last two are exothermic reactions. Because the activation energy of each reaction in this path is very high, this step is not easy to carry out compared with other reactions.

3.3. The Main Reaction Pathway Analysis

Figure 17 shows the reaction process analysis for the whole reaction. Under anaerobic conditions, the SCR process could produce the reaction $\sigma - NH_2 + NO(g) \rightarrow \sigma - NH_2NO \rightarrow \sigma - N_2 + \sigma - H_2O$, known as the E-R mechanism. The rate-determination step is the decomposition process of NHNO, and the active energy barrier can reach 55.9 kcal/mol. The same phenomenon also occurs on MnO_x/SiO_2 catalyst surfaces, where the energy barrier is about 66.89 kcal/mol [43]. There is little difference between the two, which also shows the correctness of the calculation. The lattice oxygen plays a major role in the dehydrogenation of NH_3, but there remains H left to form hydroxyl that can be oxidized by oxygen to keep the surface active. When O_2 is present, it can be absorbed and decomposed to active O on the Mn site. The NO can be oxidized to NO_2 and NO_3^-, and then participate in the rapid SCR process, which is known as the L-H mechanism. NH_4^+ can also appear because of the existence of hydroxyl, and can also react with NO to form NH_2NO and then decompose. This process is similar to that observed for V-based catalysts [24]. There are three ways to realize this process, according to the different types of surface hydroxyl groups. When active O exists on the surface, the process can be promoted because the energy barrier of every step is reduced greatly, and this also shows that O_2 plays an important role in the SCR reaction. In conclusion, both the E-R mechanism and the L-H mechanism exist on the $LaMnO_3$ catalyst surface.

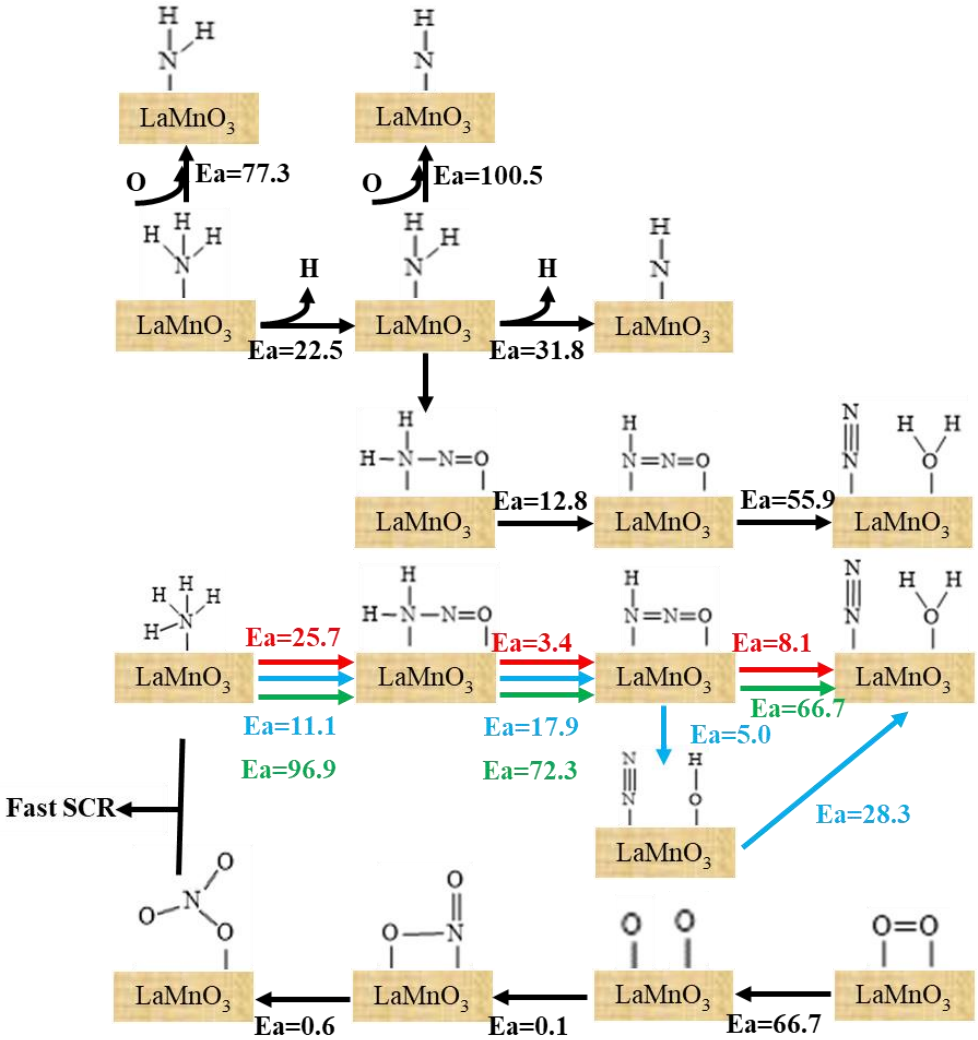

Figure 17. The reaction process analysis for NH_3-SCR of NO with $LaMnO_3$ catalyst.

4. Conclusions

The NH_3 molecule can first be absorbed on the $LaMnO_3$ catalyst surface, then it can be oxidized by lattice oxygen to form NH_2. The NH_3 can react with NO to form NH_2NO and then decompose to N_2 and H_2O. Within the process, NHNO is an intermediate and its decomposition is the rate-determining step. When O_2 exists in the atmosphere, it can be absorbed and decomposed into two active O atoms. NO can be oxidized to NO_3^- and then participate in the rapid SCR process. NH_4^+ can also appear because of the existence of hydroxyl, and can also react with NO to form NH_2NO and then decompose. There are three ways to realize this process, according to the different types of surface hydroxyl groups. When active O exists on the surface, the process can be promoted greatly as the energy barrier of every step is significantly reduced.

Author Contributions: Conceptualization, D.R. and S.L.; methodology, K.G.; validation, Z.Z., S.L.; formal analysis, D.R., Y.L. and K.W.; investigation, Y.L., X.G.; resources, S.L.; data curation, S.L., X.G.; writing—original draft preparation, D.R., K.W.; writing—review and editing, D.R.; supervision, S.L.; project administration, S.L.; funding acquisition, S.L. All authors have read and agreed to the published version of the manuscript.

Funding: Financial support for this project from the Natural Science Foundation of Shandong Province, China, (ZR2021QE295) and 2020 science and technology project of Qingdao West Coast New Area (2020-35), with grateful acknowledgment.

Institutional Review Board Statement: Not applicable.

Informed Consent Statement: Not applicable.

Data Availability Statement: Exclude this statement.

Conflicts of Interest: The authors declare no conflict of interest.

References

1. Heck, R.M. Catalytic abatement of nitrogen oxides–stationary applications. *Catal. Today* **1999**, *4*, 519–523. [CrossRef]
2. Skalska, K.; Miller, J.; Ledakowicz, S. Trends in NO(x) abatement: A review. *Sci Total Environ.* **2010**, *408*, 3976–3989. [CrossRef] [PubMed]
3. Shi, Y.; Xia, Y.-F.; Lu, B.-H.; Liu, N.; Zhang, L.; Li, S.-J.; Li, W. Emission inventory and trends of NO x for China, 2000–2020. *J. Zhejiang Univ. Sci. A* **2014**, *15*, 454–464. [CrossRef]
4. Müller, J.-F. Geographical distribution and seasonal variation of surface emissions and deposition velocities of atmospheric trace gases. *J. Geophys. Res. Atmos.* **1992**, *97*, 3787–3804. [CrossRef]
5. Forzatti, P. Present status and perspectives in de-NOx SCR catalysis. *Appl. Catal. A Gen.* **2001**, *222*, 221–236. [CrossRef]
6. Busca, G.; Lietti, L.; Ramis, G.; Berti, F. Chemical and mechanistic aspects of the selective catalytic reduction of NO_x by ammonia over oxide catalysts: A review. *Appl. Catal. B Environ.* **1998**, *18*, 1–36. [CrossRef]
7. Woo, Z.; Liu, S.I. Recent Advances in Catalytic $DeNO_X$ Science and Technology. *Catal. Rev.* **2006**, *48*, 43–89.
8. Forzatti, P. Environmental catalysis for stationary applications. *Catal. Today* **2000**, *62*, 51–65. [CrossRef]
9. Koh, H.L.; Lee, S.H.; Kim, K.L. The Effect of MoO_3 Addition to V_2O_5/Al_2O_3 Catalysts for the Selective Catalytic Reduction of NO by NH_3. *React. Kinet. Catal. Lett.* **2000**, *71*, 239–244. [CrossRef]
10. Zhu, H.Y.; Zhang, P.F.; Dai, S. Recent advances of Lanthanum based perovskite oxides for catalysis. *ACS Catal.* **2015**, *5*, 6370–6385. [CrossRef]
11. Royer, S.; Duprez, D.; Can, F.; Courtois, X.; Batiot-Dupeyrat, C.; Laassiri, S.; Alamdari, H. Perovskites as substitutes of noble metals for heterogeneous catalysis: Dream or reality. *Chem. Rev.* **2014**, *114*, 10292–10368.
12. PENAMA; FIERROJLG. Chemical structures and performance of perovskite oxides. *Chem. Rev.* **2001**, *101*, 1981–2018. [CrossRef] [PubMed]
13. Liu, X.; Yin, Y.; Yao, C.; Zuo, S.; Lu, X.; Luo, S.; Ni, C. $La_{1-x}Ce_xMnO_3$ attapulgite nanocomposites as catalysts for NO reduction with NH_3 at low temperature. *Particuology* **2016**, *26*, 66–72. [CrossRef]
14. Zhang, R.D.; Luo, N.; Yang, W.; Liu, N.; Chen, B. Low-temperature selective catalytic reduction of NO with NH_3 using perovskite-type oxides as the novel catalysts. *J. Mol. Catal. A Chem.* **2013**, *371*, 86–93. [CrossRef]
15. Guo, J.; Shi, X.; Fan, A.; Li, J.; Chu, Y.; Yuan, S. Study on the Preparation and Denitration Performance of Ce Modified La–Mn Perovskite Catalyst. *Adv. Eng. Sci.* **2021**, *4*, 233–239.
16. Wang, R.; Gui, K.; Liang, H. Effect of Ce-doped on performance of supported perovskite catalyst $LaMnO_3$/hematite for SCR of NO by NH_3. *Chem. Ind. Eng. Process* **2016**, *35*, 192–199.

17. Ramis, G.; Larrubia, M.A.; Busca, G. On the chemistry of ammonia over oxide catalysts: Fourier transform infrared study of ammonia, hydrazine and hydroxylamine adsorption over iron–titania catalyst. *Top. Catal.* **2000**, *11–12*, 161–166. [CrossRef]
18. Gallardo, J.; Escribano, A.; Ramis, V.S. An FT-IR study of ammonia adsorption and oxidation over anatase-supported metal oxides. *Appl. Catal. B Environ.* **1997**, *13*, 45–58.
19. Yang, S.; Wang, C.; Li, J.; Yan, N.; Ma, L.; Chang, H. Low temperature selective catalytic reduction of NO with NH_3 over Mn–Fe spinel: Performance, mechanism and kinetic study. *Appl. Catal. B Environ.* **2011**, *110*, 71–80. [CrossRef]
20. Zhang, Y.B.; Wang, D.Q.; Wang, J.; Chen, Q.; Zhang, Z.; Pan, X.; Miao, Z.; Zhang, B.; Wu, Z.; Yang, X. $BiMnO_3$ perovskite catalyst for selective catalytic reduction of NO with NH_3 at low temperature. *Chin. J. Catal.* **2012**, *33*, 1448–1454. [CrossRef]
21. Koebel, M.; Elsener, M.; Madia, G. Reaction pathways in the selective catalytic reduction process with NO and NO_2 at low temperatures. *Ind. Eng. Chem. Res.* **2001**, *40*, 52–59. [CrossRef]
22. Shi, H.Y.; Li, X.Z.; Xia, J.W.; Lu, X.; Zuo, S.; Luo, S.; Yao, C. Sol-gel synthesis of $LaBO_3$/attapulgite (B=Mn, Fe, Co, Ni) nanocomposite for NH_3-SCR of NO at low temperature. *J. Inorg. Organomet. Polym. Mater.* **2017**, *27*, 166–172. [CrossRef]
23. Tuo, K.; Zhang, P.; Wang, L.; Huang, H.Y. Perovskite catalysts for selective catalytic reduction of NO_x with NH_3. *J. Huazhong Agric. Univ.* **2020**, *5*, 26–34.
24. Soyer, S.; Uzun, A.; Senkan, S.; Onal, I. A quantum chemical study of nitric oxide reduction by ammonia (SCR reaction) on V2O5 catalyst surface. *Catal. Today* **2006**, *118*, 268–278. [CrossRef]
25. Sun, C.; Dong, L.; Yu, W.; Liu, L.; Li, H.; Gao, F.; Chen, Y. Promotion effect of tungsten oxide on SCR of NO with NH3 for the V2O5–WO3/Ti0.5Sn0.5O2 catalyst: Experiments combined with DFT calculations. *J. Mol. Catal. A Chem.* **2011**, *346*, 29–38. [CrossRef]
26. Li, X.; Li, Q.; Zhong, L. DFT Analysis of the Reaction Mechanism for NH3 -SCR of NOx over Mn/γ-Al2O3 Catalyst. *J. Phys. Chem. C* **2019**, *123*, 25185–25196. [CrossRef]
27. Anstrom, M.; Topsøe, N.-Y.; Dumesic, J.A. Density functional theory studies of echanistic aspects of the SCR reaction on vanadium oxide catalysts. *J. Catal.* **2003**, *213*, 115–125. [CrossRef]
28. Yan, X.; Liu, J.; Yang, Y.; Wang, Z.; Zheng, Y. A catalytic reaction scheme for NO reduction by CO over Mn-terminated $LaMnO_3$ perovskite: A DFT study. *Fuel Process. Technol.* **2021**, *216*, 106798. [CrossRef]
29. Gavin, A.L.; Watson, G.W. Modelling oxygen defects in orthorhombic $LaMnO_3$ and its low index surfaces. *Phys. Chem. Chem. Phys.* **2017**, *19*, 24636–24646. [CrossRef]
30. Wang, Z.; Liu, J.; Yang, Y.; Yu, Y.; Yan, X.; Zhang, Z. Insights into the catalytic behavior of LaMnO3 perovskite for Hg0 oxidation by HCl. *J. Hazard. Mater.* **2020**, *383*, 121156. [CrossRef]
31. Wang, Y.; Chen, L.; Cao, H.; Chi, Z.; Chen, C.; Duan, X.; Xie, Y.; Qi, F.; Song, W.; Liu, J.; et al. Role of oxygen vacancies and Mn sites in hierarchical Mn_2O_3/$LaMnO_3$-δ perovskite composites for aqueous organic pollutants decontamination. *Appl. Catal. B Environ.* **2019**, *245*, 546–554. [CrossRef]
32. Ren, D.; Gui, K.; Gu, S. Mechanism of Improving the SCR NO Removal Activity of Fe_2O_3 Catalyst by Doping Mn. *J. Alloy. Compd.* **2021**, *867*, 158787. [CrossRef]
33. Ren, D.; Gui, K.; Gu, S. Quantum chemistry study of SCR-NH3 nitric oxide reduction on Ce-doped γFe_2O_3 catalyst surface. *Mol. Catal.* **2021**, *502*, 111373. [CrossRef]
34. Delley, B. From molecules to solids with the DMol3 approach. *J. Chem. Phys.* **2000**, *113*, 7756–7764. [CrossRef]
35. Bergner, A.; Dolg, M.; Küchle, W.; Stoll, H.; Preuß, H. Ab initio energy-adjusted pseudopotentials for elements of groups. *Mol. Phys.* **1993**, *80*, 1431–1441. [CrossRef]
36. Yang, Y.; Liu, J.; Zhang, B.; Liu, F. Mechanistic studies of mercury adsorption and oxidation by oxygen over spinel-type $MnFe_2O_4$. *Hazard. Mater.* **2017**, *321*, 154–161. [CrossRef] [PubMed]
37. Ren, D.; Gui, K.; Gu, S.; Wei, Y. Study of the nitric oxide reduction of SCR-NH_3 on nano-γFe_2O_3 catalyst surface with quantum chemistry. *Appl. Surf. Sci.* **2020**, *509*, 144659. [CrossRef]
38. Halgren, T.A.; Lipscomb, W.N. The synchronous-transit method for determining reaction pathways and locating molecular transition states. *Chem. Phys. Lett.* **1997**, *49*, 225–232. [CrossRef]
39. Liu, Y.; Liu, J.; Lin, Y.S.; Chang, M. Effects of water vapor and trace gas impurities in flue gas on CO_2/N_2 separation using ZIF-68. *Phys. Chem. C* **2014**, *118*, 6744–6751. [CrossRef]
40. Ramis, G.; Angeles Larrubia, M. An FT-IR study of the adsorption and oxidation of N-containing compounds over Fe_2O_3/Al_2O_3 SCR catalysts. *J. Mol. Catal. A Chem.* **2004**, *215*, 161–167. [CrossRef]
41. Yang, Y.; Liu, J.; Wang, Z.; Liu, F. A skeletal reaction scheme for selective catalytic reduction of NOx with NH_3 over CeO_2/TiO_2 catalyst. *Fuel Process. Technol.* **2018**, *174*, 17–25. [CrossRef]
42. Yao, H. Periodic DFT study on mechanism of selective catalytic reduction of NO via NH_3 and O_2 over the V_2O_5 (001) surface: Competitive sites and pathways. *J. Catal.* **2013**, *305*, 67–75. [CrossRef]
43. Gu, S.; Gui, K.; Ren, D.; Wei, Y. The effects of manganese precursors on NO catalytic removal with $MnOxSiO_2$ catalyst at low temperature. *React. Kinet. Mech. Catal.* **2020**, *130*, 195–215. [CrossRef]
44. Gu, S.; Gui, K.; Ren, D.; Wei, Y. Understanding the adsorption of NH_3, NO and O_2 on the $MnOxSiO_2$ β-cristobalite (101) surface with density functional theory. *React. Kinet. Mech. Catal.* **2020**, *130*, 741–751. [CrossRef]

45. Savara, A.; Li, M.-J.; Sachtler, W.M.; Weitz, E. Catalytic reduction of NH_4NO_3 by NO: Effects of solid acids and implications for low temperature De-NOx processes. *Appl. Catal. B Environ.* **2008**, *81*, 251–257. [CrossRef]
46. Wang, D.; Zhang, L.; Kamasamudram, K.; Epling, W.S. In Situ-DRIFTS Study of Selective Catalytic Reduction of NOx by NH_3 over Cu-Exchanged SAPO-34. *ACS Catal.* **2013**, *3*, 871–881. [CrossRef]